25th Symposium on Naval Hydrodynamics
St. John's, Newfoundland and Labrador, CANADA, 8-13 August 2004

Numerical and Experimental Investigation of the Hub Vortex Flow of a Marine Propeller

Moustafa Abdel-Maksoud [1], Katrin Hellwig [2], Jörg Blaurock [3]
([1]Duisburg-Essen University, [2]Potsdam Model Basin, [3]Consultant, Hamburg)

ABSTRACT

The shape of hub caps can have a strong influence on the hub vortex and the cavitation inception of this vortex. The delay or avoidance of hub vortex cavitation is important not only for navy ships but also for merchant ships. This can reduce the noise level of navy ships and avoid vibration or damage in the rudder region behind the propeller of merchant ships.

Numerical and experimental investigations were carried out to study the effect of the hub cap shape on the hub vortex. The investigations were conducted for a propeller which was arranged with three differently shaped hub caps. The experimental tests included cavitation observation model tests in a cavitation tunnel and open water tests in a cavitation tunnel and in a towing tank. LDV and PIV measurements were carried out to obtain more information on the mechanism of formation, the structure of the hub vortex and the velocity field behind the hub. Simultaneously, the velocity fields on the propeller and behind the hub were calculated for model and full-scale. The comparison between the calculated and measured results for model scale confirms that the applied numerical method is able to predict the complicated velocity field behind a propeller.

The calculated pressure coefficients of the full-scale results show a strong pressure reduction in the hub vortex region in comparison to model scale. The calculated minimum pressure-coefficient values behind the propeller confirm that the cavitation inception of the full-scale takes place much earlier than in the model scale.

INTRODUCTION

The form of the hub cap of a propeller is an integral component of the propeller geometry. During the design process of a propeller, the shape of the hub cap is rarely given considerable attention - although the shape of the hub cap may have an appreciable influence on propeller efficiency as well as on the cavitation behaviour of the hub vortex.

To achieve the high requirements of acceptable noise level of a navy ship propeller, it is important to delay all kinds of propeller cavitation including hub vortex cavitation. In some cases hub vortex cavitation may be the first to appear. The shape of the hub cap can play an important role in influencing the characteristics and intensity of the hub vortex. Therefore, when designing the shape of the hub cap, it is important to find an optimum compromise between cavitation behaviour, efficiency and other important aspects of the propeller design. For these reasons detailed information on the local flow around and behind the hub cap is needed to support the design process.

At the moment, the cavitation bucket diagram of a propeller is still determined experimentally. The extrapolation methods of model results of hub vortex inception to full-scale differ in various model basins. The prognosis of hub vortex cavitation inception for full scale is still not accurate. The reason is the difficulty of taking into account the influence of the Reynolds number, and water quality on the results.

Unclassified studies on the form of the hub cap were very limited. This could possibly be attributed to investigations being carried out within a project conducted by a propeller manufacturer. Published results cover only a very limited number of parameters (Missalek, 1966).

AIM OF STUDY

The main aims of the study were focusing on the characteristics of the flow of hub vortices and analysing the influence of the different cap shapes on the propeller efficiency. Another important aim of the study was to investigate the possibility of using CFD results to assist correlation procedures for the prognostic of the cavitation inception of the hub vortex for full-scale. For this reason, the pressure reduction in the core of hub vortex was calculated for model and full-scale.

All model tests as well as all calculations were carried out for uniform inflow condition.

OBJECTS OF RESARCH

In the present study the viscous flow on a geometry of a propeller with three different cap shapes was investigated. A 5 bladed controllable pitch propeller was selected for the investigations. The propeller has a typical radial load distribution as normally used for a navy ship to delay cavitation inception (strong de-loaded at blade tip and root). The hub diameter ratio and skew angle equal 0.2976 and 22.7° respectively. The scale ratio of the propeller model is 12. Main parameters of the propeller model (VP 1352) are:

D = 350.0 mm
Z = 5
Pm/D = 1.279
Ae/Ao = 0.72

The three hub cap shapes investigated have different characteristics. The first has a concave shape and is named CON. The second is a divergent hub cap, named DIV, and the last is a mixed form between the first and the second shape. The forward part of this hub cap is concave and the after part is divergent. Therefore, it has been named CONDIV.

The selected shapes of the hub cap are based on the results of a previous intensive investigation (Blaurock, 1987).

The geometry of the investigated propeller and the hub cap shapes are shown in Figures 1 and 2.

All numerical and experimental tests were carried out only for design pitch condition.

EXPERIMENTAL STUDY

The model tests were conducted in the cavitation tunnel of the Potsdam model basin. The cross section area of the measuring section is equal - 850 x 850 mm. The following tests were carried out: propeller open water test, observation of cavitation inception and velocity measurements using LDV and PIV methods. All tests were performed for every cap shape. The open water tests were repeated in the towing tank. The Reynolds number of the open water test varied between 0.98×10^6 and 2.4×10^6.
The velocity measurements were carried out behind the three shapes at two operation points J= 1.0 and J=1.06. For the comparison with the numerical results phase averaged values of the LDV measured data were calculated in 2 degree steps, which means that the mean values of the three velocity components were available for LDV results at 180 angular positions of the propeller (Abdel-Maksoud et. al., 2002). Similar LDV measurements were carried out with a FP propeller model also having 3 different cap shapes at two cross sections each behind the caps (Blaurock and Lammers 2001). These tests demonstrated significant differences in the velocity field caused by the different shaped caps, as also found in the present tests.

EXPERIMENTAL RESULTS

The results of the open water tests are shown in Figure 3. The measured efficiency of the propeller with CON and CONDIV hub cap are similar (η_o=0.70) (KONDIV slightly better than CON, but within the measuring accuracy). The measured efficiency of the propeller with CON and CONDIV hub cap is higher than that measured with DIV shape (o=0.67). The same results have been obtained in the towing tank.

Cavitation model tests were carried out at 63% and 42% air content. Figure 4 shows the cavitation buckets of the propeller with the three different hub cap shapes at 63% air content. The operation curve of the propeller at different thrust coefficients is also included. Hub vortex cavitation inception has been defined as the condition when cavitation occurred in 5% of the observation time. The intersection points between hub vortex cavitation buckets and the operation curve of this particular propeller show that the DIV-shape has the worst cavitation behaviour (hub vortex starts at about 20 kts). The cavitation

inception behaviour of the CONDIV-form is the best, it starts at about 29.5 kts. The cavitation inception of hub vortex of CON shape takes place at about 26 kts.

The experimental results show additionally high dependency on the thrust loading coefficient. At KT=0.25 the differences in the cavitation behaviour of the different hub cap shapes are very small, but this is an off-design operating point. According to these results, it may be concluded that under other boundary conditions (i.e. higher loaded propeller, other radial blade load distributions etc.) the most suitable hub cap form might be other than the shape found in this particular case.

First occurrence of the hub vortex cavitation with hub caps DIV and CONDIV could be observed at about 2 D to 4 D behind the cap. When decreasing the cavitation number, the position of first occurrence of the hub vortex cavitation moves towards the cap until about 0.2 D behind it.

Cavitation of hub vortex of the cap CON was observed at 0.2 D behind the hub only. The cavitation did not touch the cap at any investigated cavitation number. That is the reason why Figure 4 includes only one curve for far and close cavitation inception of the CON hub vortex. Cavitation occurred at the same time in a region extending between 0.2 D to about 3 D. The best cavitation behaviour of the CON shape was measured in this range, when the propeller was operating at J values higher than 0.8 or KT values lower than 0.25 respectively, which is the design operating range of the tested propeller.

All other cavitation types of the propeller were very similar for the three different caps.

The experimental results showed that the effect of the air content on the observed cavitation behaviour did not have the same tendency for all operation points of the propeller. At J-values of 0.8 or lower , the cavitation of the hub vortex started at higher pressure with a gas content of 63 % rather than with 42 % . At higher J-values cavitation an opposite tendency was observed, which means that hub vortex cavitation inception occurred with 63 % at lower pressure rather than with 42 %.

The results given in this paper are taken with 63% gas content.

NUMERICAL COMPUTATION

The commercial CFX-TASCflow code has been applied to solve the Reynolds-averaged Navier-Stokes equations. CFX-TASCflow is based on a conservative finite volume method. CFX-TASCflow uses a non-orthogonal, block-structured numerical grid, in conjunction with Cartesian velocity components. For a description of the application of CFX-TASCflow method for propeller flow see Abdel-Maksoud and Heinke, 2002.

The applied discretization method of the convective terms in transport equations is based on the Mass-Weighted-Skew-Upwind-Differencing method (MWS) and the Linear-Profile-Skew-Upwind differencing procedures (LPS). The accuracy of the calculated convective terms is improved with the help of the Physical Advection Correction (PAC) method.

Multi-grid technology is applied to reduce long-wavy errors and to accelerate the solution of the algebraic equation system. While the masses and three impulse conservation equations in every iteration are coupled solved, the turbulence equations are solved individually. The coupled solution of the masses and impulse conservation equations has many advantages especially for a complicated flow behaviour and it leads to a robust, reliable and quick algorithm.

To solve the Navier-Stokes equation for the propeller the solution domain is divided into two regions. The outside region is stationary and the region inside, which includes the propeller, rotates. Between the inside and the outside region a sliding non-matching interface is applied (Abdel-Maksoud and Heinke, 2002). For turbulence modelling the SST model is applied.

Especially in the separated flow region for example behind the hub, more accurate results can be achieved with the SST turbulence model. Although the calculations were carried out for a propeller in homogeneous flow, all propeller blades are considered in the study. This was necessary to focus the interaction between the root vortices of the propeller blades and the unsteady behaviour of the hub vortex flow.

The applied numerical grid Control contains about 1.3 Mio. control volumes and most of them are located in the hub region in order to capture the detail of the flow in this region. The numerical grid is

shown in Figures 1 and 5.

The applied numerical method was validated for propeller flow calculations (Abdel-Maksoud, Menter and Wuttke, 1998). It was also applied to calculate the unsteady interaction between hull and propeller (Abdel-Maksoud, Rieck and Menter, 2000).

In most of the pervious studies the main interest was the flow around the propeller blades. In the present investigation the capture of flow behind the propeller hub was main aim of the calculations. The flow in this region is very complicated due to the interaction between the root vortex of every propeller blade and the separated flow region behind the hub. The measured velocity results in model scale were used to validate the numerical results in this region.

NUMERICAL RESULTS

The calculated efficiencies of the propeller show the same tendency as the measured data. The efficiencies of the propeller with CON and CONDIV hub caps are close to each other and much higher than that with DIV shape. The absolute efficiency differs from those measured. This can be explained by the fact that the number of grid cells on the outer radii of the propeller blades was kept to a minimum in order to be able to apply higher grid resolution at the inner radii of the propeller blades and behind the hub. The total number of cells was kept below a certain limit to enable a large number of numerical computations to be carried out within an acceptable time.

The flow behaviour around the CONDIV shape can be seen in the Figures 6-8. The low pressure regions in the flow are shown in Figure 6. These regions are located on the suction side of the propeller blade and directly behind the hub cap as well as at a certain distance behind it. At this location the root vortices are coincided together and form a strong hub vortex with low pressure region. The streamlines near the root region of the blades are shown in Figure 7. The swirl component dominates the flow in this region. A separated flow region is located directly behind the hub cap. The shape of the streamlines is changed suddenly behind the separated flow region as shown in Figure 8.

A comparison of measured and calculated axial velocity component in a longitudinal section along the rotation axis is included in Figure 9. Results of the LDV and the PIV measurements as well as the numerical calculations for model scale are presented in this figure. The axial velocity component is normalised by the parallel inflow velocity. The dark blue areas or contour lines indicate separated flow. The red areas mean that axial velocity component is equal to 90% of the normalised velocity or higher.

Good agreement was achieved between calculated and measured velocity contours for each hub cap. While the contours of the numerical and the PIV results are for one angular position, the results of LDV measurements are the mean value of many measured data at the same angular position. This is the reason for the unsteady character of the numerical and the PIV results.

The LDV, PIV and numerical results show that the shape variant DIV has the largest separation flow region behind the hub cap. This region exists along the axis of rotation of the propeller for all investigated hub cap forms. The smallest separation flow region is located behind the hub cap CONDIV.

The measured LDV velocity components and those calculated were compared at different cross sections plans behind the propeller. Figure 10 shows the results for the axial velocity component at 0.1 D behind the propeller. The results of the LDV measurements are plotted in black and the numerical results are plotted in blue.

The calculation results of the three geometry forms at r/R= 0.7 agree well with those measured. In this cross section, the maximum axial velocity component of the propeller flow varies between 1.2 - 1.4 of the inflow velocity. The highest acceleration occurs behind the shape DIV. This is because the increase of the diameter of the hub cap behind the propeller blade reduces the available area for propeller stream. This may be the reason for the reduced propeller efficiency in combination with the hub cap shape DIV.

In the region very close to the root of the propeller blades r/R= 0.16, the flow is de-accelerated. The calculated and the measured values show back flow region behind the form variants DIV and CON. The axial velocity component behind the form CONDIV is still very low but it is higher than that behind the other two shapes.

The DIV shape produces a large separation region behind it which enables the blade root vortices to keep distance from each other for a long distance behind the hub cap in comparison to CONDIV. Behind CONDIV shape the individual root vortices may unify with each other and cause as a consequence locally higher circulation, which leads to lower pressure, and hence earlier cavitation inception. Furthermore, the flow becomes extremely intermittent. Small differences in the local geometry of the model propeller blades may initiate small differences in the flow downstream of the different blades. However, the calculation results show less intermittent flow. This is due to the fact that the geometry of the propeller blades for the all five blades is identical. The capturing of this intermittent behaviour of the flow behind the hub was the reason for considering all propeller blades in the computations and for applying a fine grid behind the hub.

Several factors may be responsible for the differences between the model test and numerical results. Many sources of uncertainty can reduce the accuracy of the results of numerical computations for separated flow, such as: discretization errors due to a limited number of control volumes used and applied discretization scheme and modelling error due to the limited accuracy of the applied turbulence model and the neglecting of the effect of the air content on the flow in the computations.

An important source of uncertainty in carrying out cavitation model tests is the difficulty to define exactly the cavitation inception by observation. The quality of the results depends on the experience of the observer. Furthermore, there is a hysteresis effect concerning the cavitation inception. This means the cavitation inception pressure depends on the experimental procedure i.e. whether the pressure in the cavitation tunnel decreases or increases during the model test. Even after taking all these shortcomings into account, the results of the calculations seem very promising.

CORRELATION BETWEEN THE CALCULATED RESULTS FOR MODEL AND FULL-SCALE

The velocity distribution in the longitudinal section along the rotation axis is shown for model and full-scale in Figure 11 and 12. The shape of the separated flow region behind all investigated hub cap shapes in the model scale shows a different characteristic as compared to the full-scale study.

At full-scale in all investigated hub cap shapes, there is a ring-shaped vortex directly behind the edge of the hub cap. The diameter of this ring is proportional to the diameter of the hub cap at the end. The numerical results of the model scale show that the centre line of the hub vortex does not lie on the axis of rotation of the propeller, but oscillates around this axis with an increasing amplitude. The oscillation of the hub vortex in the model scale is a result of strong interaction between the root vortices of propeller blades due to the short distance between them. A small disturbance is sufficient for two root vortices to coincide together. This disturbs the symmetry of the system and therefore it starts to oscillate. The oscillation of the hub vortex of CON and CONDIV shapes is stronger than that of the DIV.

Figure 13 shows the contours of the normalised pressure p_{NORM} of the three hub cap forms in the longitudinal section along the axis of rotation.

$$p_{Norm} = \frac{p}{0.5 \cdot \rho \cdot \left(V^2 + \left(0.7 \cdot D \cdot n \cdot \pi\right)^2\right)} \qquad (1)$$

The pressure reduction on the suction side of the blades, the increase of pressure on the pressure side and the low pressure region behind the hub cap can be seen in Figure 13. The comparison of the numerical results for the model and full-scale shows that the pressure contours of the full-scale are much smoother than those in the model. The reduction of normalised pressure behind the full-scale is much higher than in the model. This effect is much stronger for the hub cap DIV in comparison to the other two shapes.

Table 1 includes the normalised minimum pressure in the centre of the hub vortices. The numerical results show that the pressure reduction in the full-scale is much stronger than in the model scale. The calculated lowest pressure reduction for the first operation point at full-scale takes place with the hub cap CON. That is the case in both model and full-scale.

The calculated normalised pressure in the centre of the hub vortices confirms that the use of the McCormick formula is necessary for the extrapolation of the experimental results to the full-scale experiments (McCormick, 1962).

The calculated pressure values were used to determine the exponent of McCormick formula as shown in Table 1.

$$\frac{(p_{Norm})_{\text{full-scale}}}{(p_{Norm})_{\text{model}}} = \left[\frac{(Rn)_{\text{full-scale}}}{(Rn)_{\text{model}}}\right]^{m} \qquad (2)$$

Table 1: Calculated normalised minimum pressure values in the centre of the hub vortices and the corresponding McCormick exponent.

	Model	Full-scale	Exponent
	p_{Norm}	p_{Norm}	m
DIV	-0.06	-0.225	0.40
CON	-0.045	-0.131	0.32
CONDIV	-0.058	-0.155	0.31
		mean value	0.34

The mean exponent value was determined for one propeller geometry only and for one radial thrust loading distribution. Therefore, the value of the exponent *m* may be not applicable for all propeller and hub cap geometry.

CONCLUSIONS AND RECOMMENDATIONS

The effect of the shape of the hub cap on propeller efficiency as well as on hub vortex cavitation inception is significant. It is therefore recommended to pay more attention to the shaping of the cap of the hub, especially when operating with low noise is important.

The results of the study confirm that the highly sophisticated velocity- and pressure field behind the hub of an operating propeller can be predicted by applying numerical methods for viscous flow calculation. These methods are a good tool for predicting the pressure reduction in the hub vortex and therefore it is possible to apply CFD-methods to find out the most suitable hub cap shape. This is valid for model as well as for full-scale conditions.

Furthermore, the results of the calculations showed that the cavitation inception of hub vortices with model tests (at low Reynolds numbers) should be extrapolated to full scale using the formula as suggested by McCormic.

Differently shaped hub caps may have a significant influence on propeller efficiency. A divergent cap has a negative influence. A moderate convergent influence such as CON and the special shape CONDIV may have a positive influence.

This statement is valid for propellers with a relatively high hub diameter ratio, which is the typical case for CP propellers. For fixed pitch propellers having an hub diameter ratio of 0.2 or even less the difference between different cap shapes can be expected to be small and may be ignored. Hence the cap shape for such propellers should be selected only with regard to hub vortex cavitation inception of the hub vortex.

ACKNOWLEDGEMENT

The authors would like to express their gratitude to the Federal Office of Defence, Technology and Procurements, Department Ships and Naval Equipment for the support of this study.

LIST OF SYMBOLS

Ae/Ao	=	expanded area ratio of the propeller
D	=	propeller diameter
dh	=	hub diameter
J	=	advance ratio $= V/(n*D)$
KT	=	propeller thrust coefficient
KQ	=	propeller torque coefficient
kn	=	knots
m	=	exponent in McCormics formula
n	=	number of revolutions
Pm	=	mean pitch of propeller
PS	=	pressure side
p_{Norm}	=	normalised pressure
r	=	local radius
R	=	propeller radius $= D/2$
Rn	=	Reynolds number
SS	=	suction side
V	=	mean inflow velocity
Z	=	number of propeller blades
η_o	=	propeller efficiency $= J/(2*\pi) * KT/KQ$
ρ	=	density of fluid (water)
σ	=	cavitation number

REFERENCES

Abdel-Maksoud, M., Menter, F. R., Wuttke, H., "Viscous Flow Simulations for Conventional and High Skew Marine Propellers," Ship Technology Research, Vol. 45, No. 2, 1998.

Abdel-Maksoud, M., Rieck, K., Menter, F. R., "Unsteady Numerical Investigation of the Turbulent Flow Around The Container Ship Model (KCS) with and without Propeller," Gothenburg 2000, A Workshop on Numerical Ship Hydrodynamics, Gothenburg, Sweden, 2000.

Abdel-Maksoud, M., Heinke, H., "Scale effects on Ducted Propellers," 24th Symposium on Naval Hydrodynamics, Fukuoka, Japan, July 2002

Abdel-Maksoud, M., Hellwig, K., Blaurock, J., Schmidt, D., Jaksic, D., "Correlation of Propeller Cavitation – Design of Hub Cap," Potsdam Model Basin, Report No. 2839, , October 2002 (in German, Classified).

Blaurock, J., "Influence of the Propeller Hub Cap Shape on Hub Vortex Cavitation," 6. US-GE-Hydroacoustics Symposium, Annapolis, MD.,1987 (Classified).

Blaurock, J., Lammers, G., "Velocity Field behind the Propeller Hub with different shaped Caps," HSVA Report No. 1559, Hamburg, Sept. 2001 (in German)

McCormic, jr. B.W. "On Cavitation Produced by a Vortex Trailing from a Lifting Surface," Journal of Basic Engineering, Sept. 1962

Missalek, R., "Influence of the Form of the Hub Cap on Open water and Cavitation Characteristic," VWS Berlin, Report Nr. 325,1966 (in German).

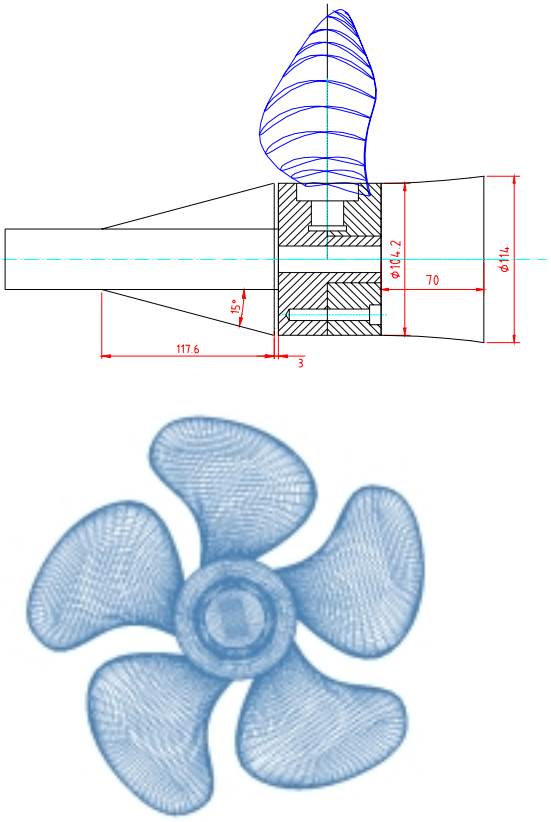

Figure 1: Investigated propeller geometry

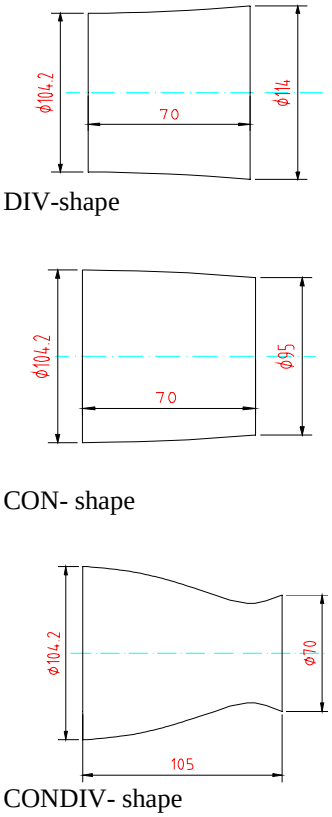

Figure 2: Geometry of hub cups

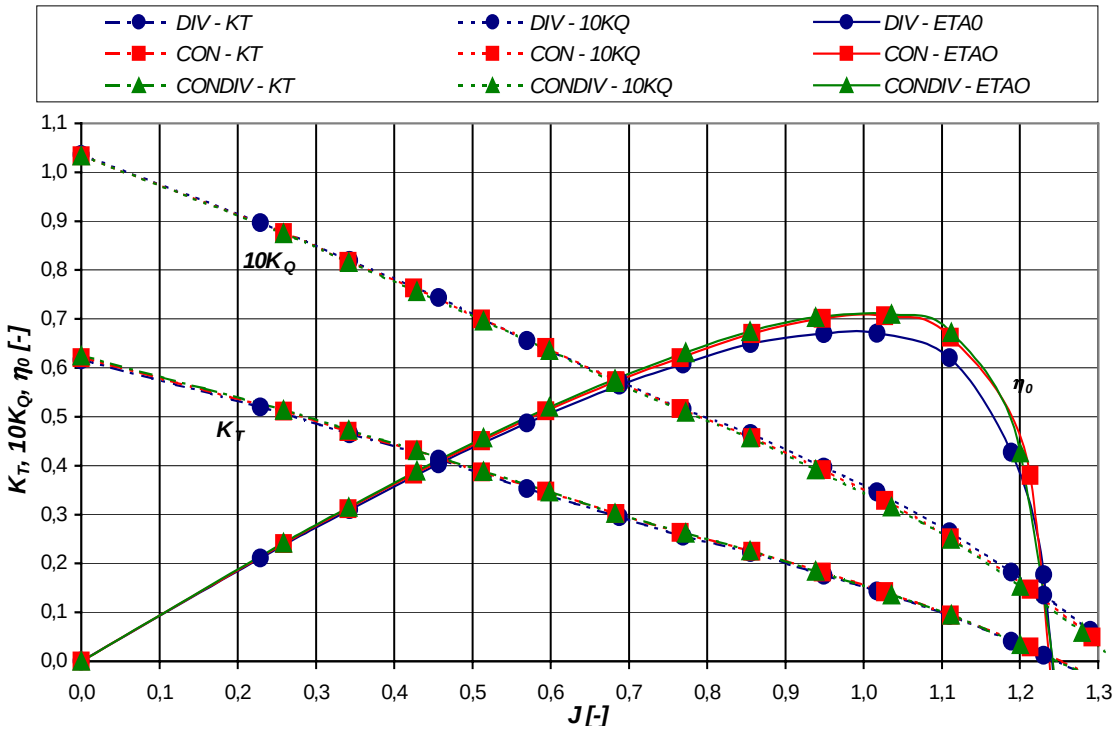

Figure 3: Open water test

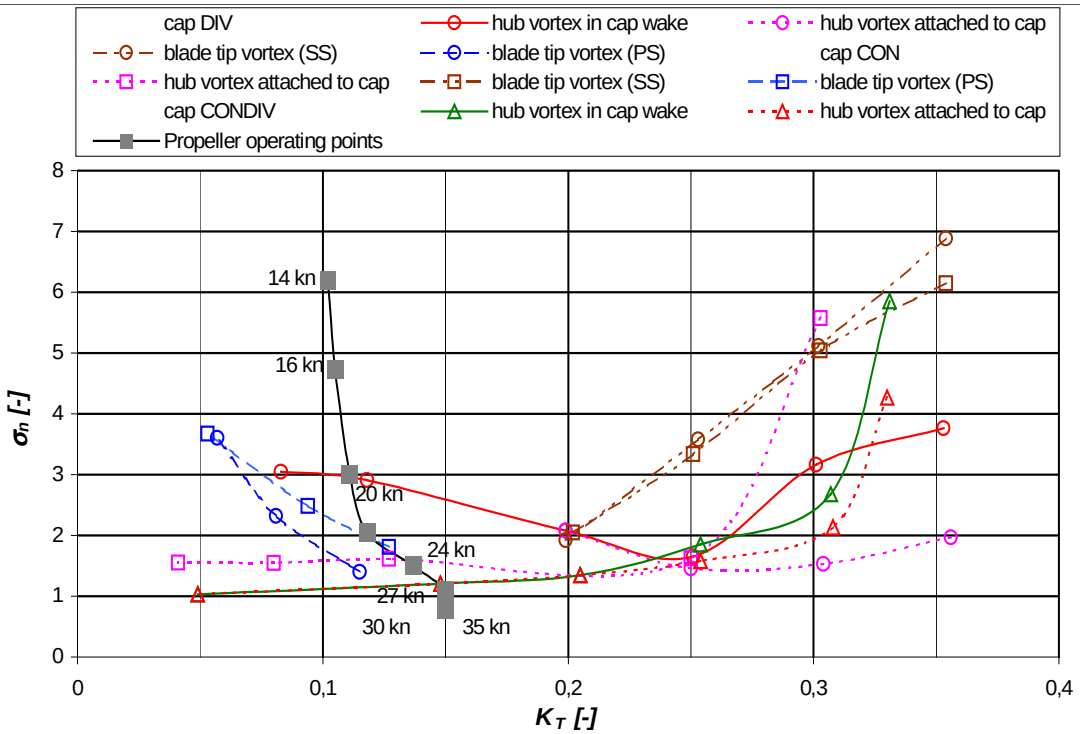

Figure 4: Cavitation bucket curves

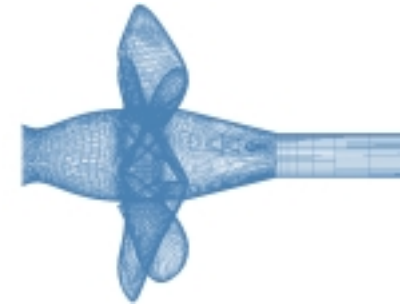

Figure 5: Numerical grid

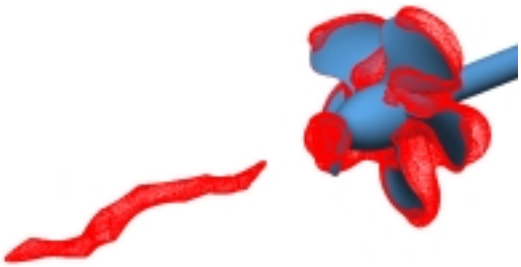

Figure 6: Low pressure regions

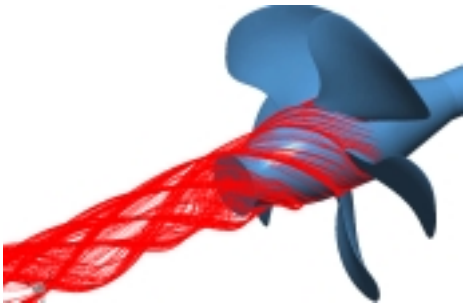

Figure 7: Streamlines in the root region

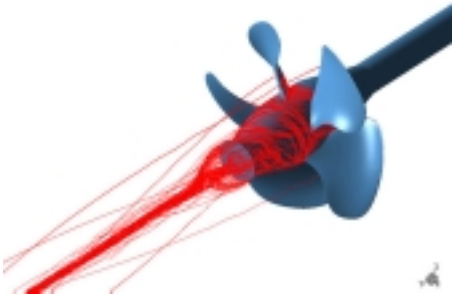

Figure 8: Streamlines of the hub vortex

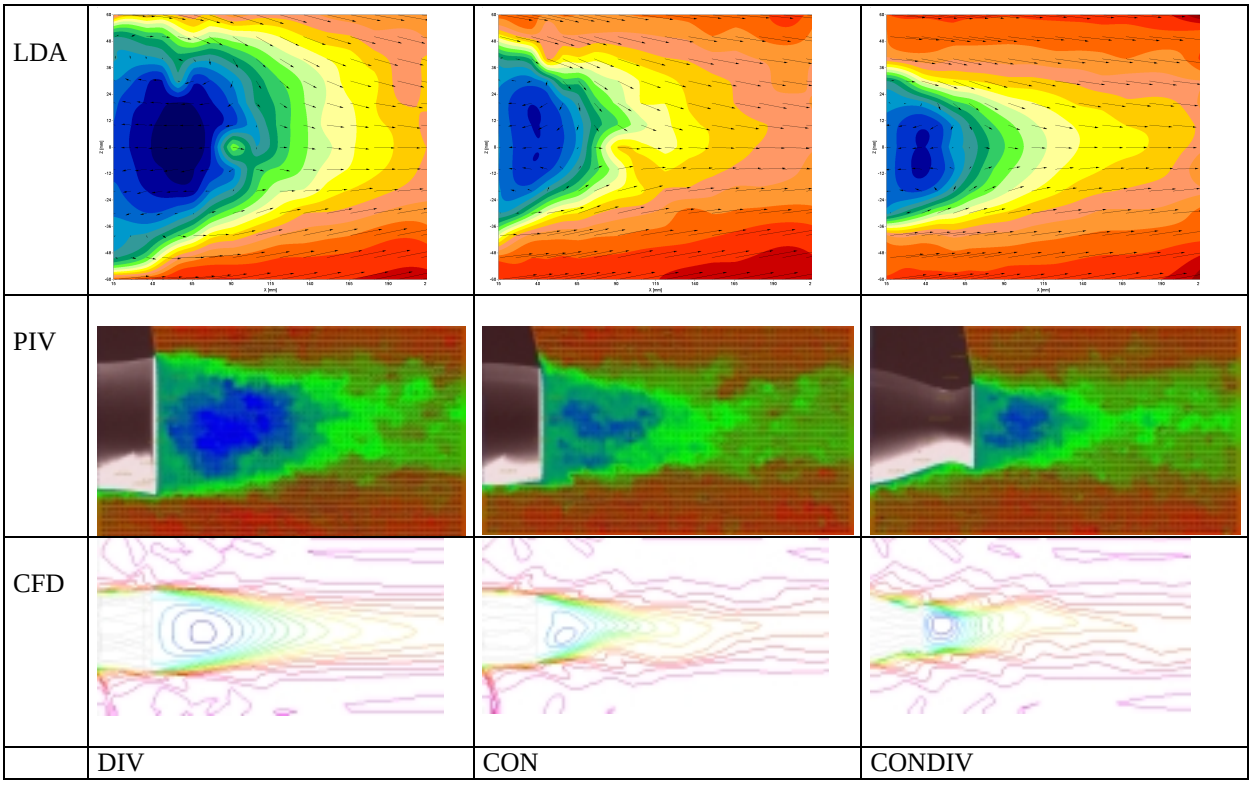

Figure 9: Comparison of measured and calculated axial velocity component, longitudinal section

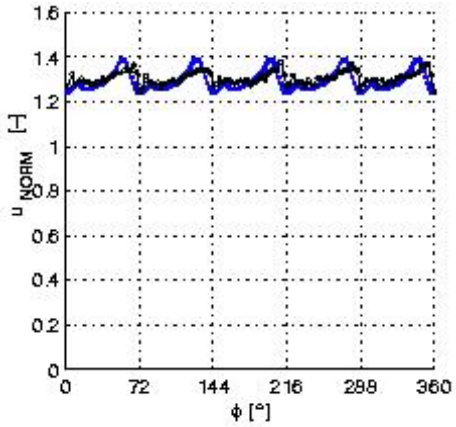

DIV, *r/R*=0.71

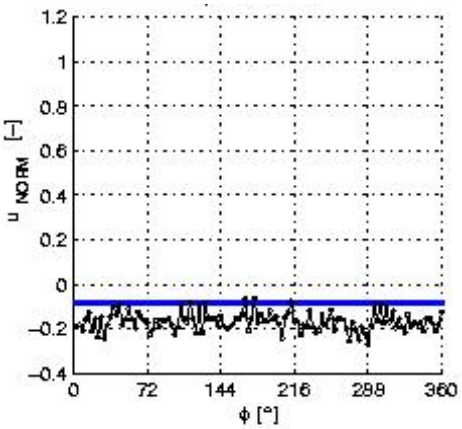

DIV, *r/R*=0.16

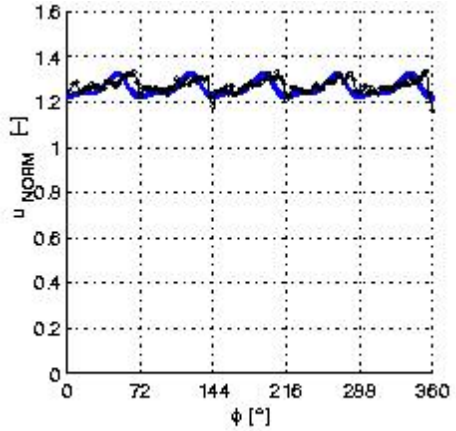

CON, *r/R*=0.71

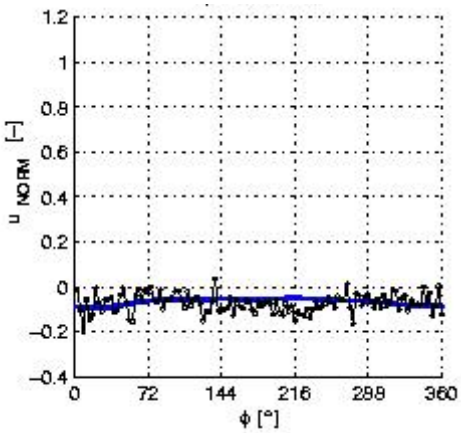

CON, *r/R*=0.16

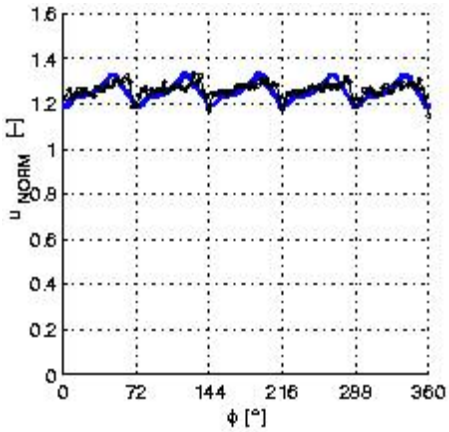

CONDIV, *r/R*=0.71

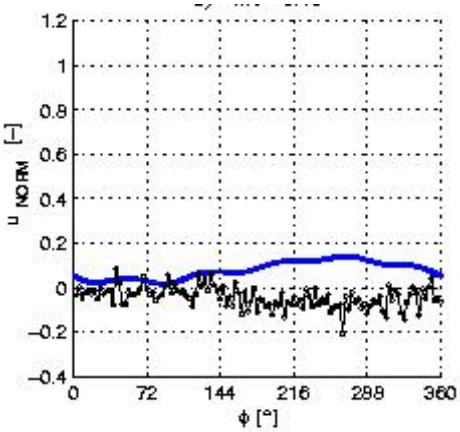

CONDIV, *r/R*=0.16

Figure 10: Comparison of measured and calculated axial velocity component, cross section

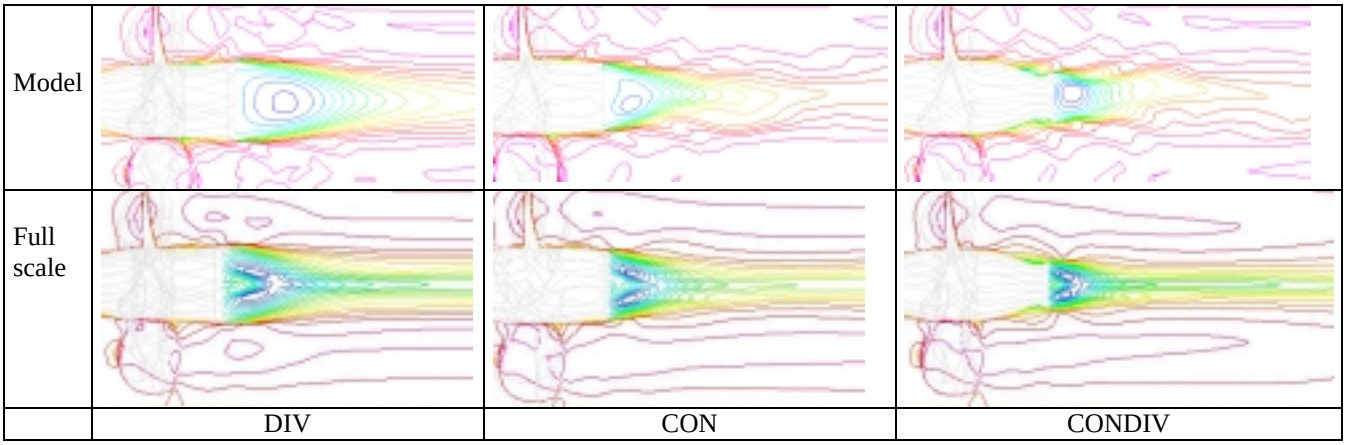

Figure 11: Comparison of calculated axial velocity contours for model and full-scale

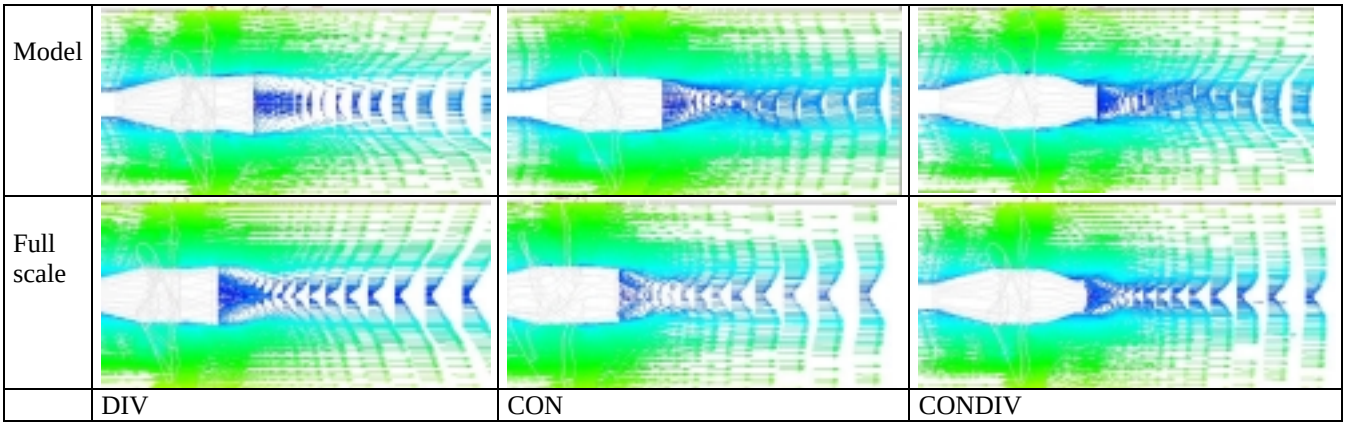

Figure 12: Comparison of calculated axial velocity vectors for model and full-scale

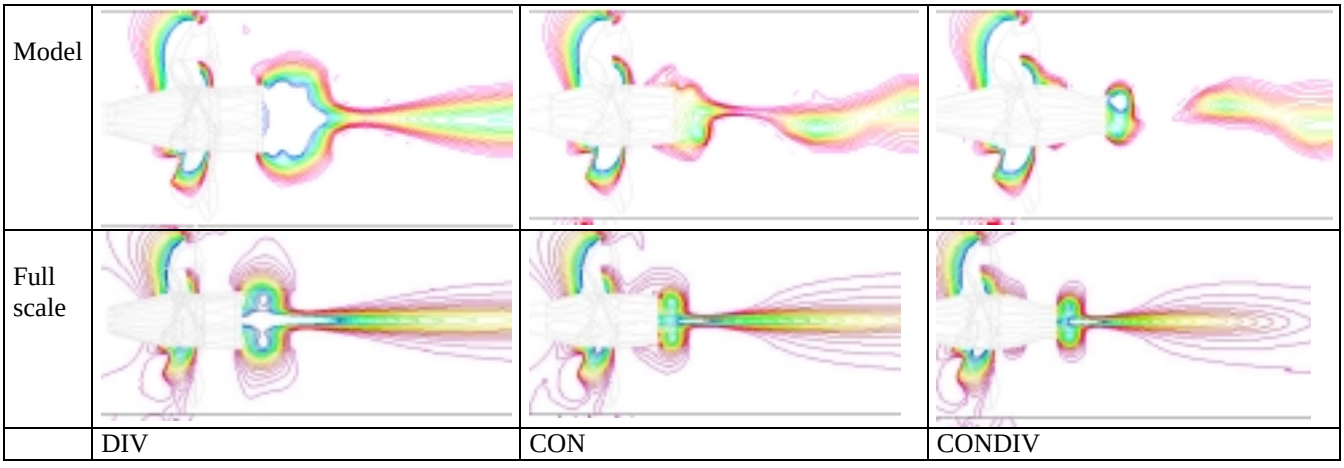

Figure 13: Comparison of calculated pressure field for model and full scale